The Canadian Mineralogist
Vol. 49, pp. 623-638 (2011)
DOI: 10.3749/canmin.49.2.623

LEAD–ANTIMONY SULFOSALTS FROM TUSCANY (ITALY). XI. THE NEW MINERAL SPECIES PARASTERRYITE, $Ag_4Pb_{20}(Sb_{14.5}As_{9.5})_{\Sigma 24}S_{58}$, AND ASSOCIATED STERRYITE, $Cu(Ag,Cu)_3Pb_{19}(Sb,As)_{22}(As–As)S_{56}$, FROM THE POLLONE MINE, TUSCANY, ITALY †

YVES MOËLO§

Institut des Matériaux Jean Rouxel, UMR 6502, CNRS, Université de Nantes, 2, rue de la Houssinière, F–44 322 Nantes Cedex 3, France

PAOLO ORLANDI

Dipartimento di Scienze della Terra, Università di Pisa, Via S. Maria 53, I–56126 Pisa, Italy

CATHERINE GUILLOT-DEUDON

Institut des Matériaux Jean Rouxel, UMR 6502, CNRS, Université de Nantes, 2, rue de la Houssinière, F–44 322 Nantes Cedex 3, France

CRISTIAN BIAGIONI

Dipartimento di Scienze della Terra, Università di Pisa, Via S. Maria 53, I–56126 Pisa, Italy

WERNER PAAR

Department of Materials Engineering and Physics (Division of Mineralogy), University of Salzburg, Hellbrunnerstrasse 34, A–5020 Salzburg, Austria

MICHEL EVAIN

Institut des Matériaux Jean Rouxel, UMR 6502, CNRS, Université de Nantes, 2, rue de la Houssinière, F–44 322 Nantes Cedex 3, France

ABSTRACT

The new mineral species parasterryite has been discovered in the Pollone barite – pyrite – (Pb–Zn–Ag) deposit at Valdicastello Carducci, near Pietrasanta, in the Apuan Alps, Tuscany, Italy. It forms acicular crystals up to 4 × 0.3 mm in vugs in quartz–barite veins. Sterryite (second world occurrence) also is present. The associated sulfides and sulfosalts are pyrite, sphalerite and various Sb–As sulfosalts. Parasterryite is black and metallic. Under the microscope, it is white with weak pleochroism; anisotropism is distinct, with greenish and brownish tints. Data on maximum and minimum reflectances for the COM wavelengths are [λ (nm), R_{air}, R_{oil} (%)]: 470: 35.1, 40.8 and 19.4, 22.2, 546: 33.5, 39.3 and 19.3, 21.7, 589: 32.7, 38.2 and 18.7, 21.1, 650: 31.4, 36.5 and 17.3, 19.5. Hardness VHN_{10} = 238 kg/mm^2. An electron-microprobe analysis gave (in wt.%, mean result of 32 spot analyses): Cu 0.09(2), Ag 4.36(6), Hg 0.15(2), Pb 47.00(18), Sb 19.57(30), As 7.73(21), S 20.56(7), total 99.46(23). A single-crystal X-ray study of parasterryite indicates monoclinic symmetry, space group $P2_1/c$, with a 8.3965(5), b 27.9540(4), c 43.8840(13) Å, β 90.061(12)°, V = 10300(3) Å^3. The main powder-diffraction lines [d in Å(I)(hkl)] are: 3.62(100)(075, 01$\underline{1}$2, 234, $\overline{2}$34), 3.42(45)(244, $\overline{2}$44), 3.35(95)(01$\underline{1}$3), 3.23(65)(078), 3.01(45)(239, $\overline{2}$39), 2.945(85)(088), 2.885(80), 1.916(45). The name *parasterryite* reflects its close structural relationship with sterryite. Sterryite is more abundant than parasterryite. Electron-microprobe analyses of two samples gave: 1) Sb-rich sterryite (wt.%): Cu 1.27(1), Ag 2.19(11), Hg 0.55(5), Tl 0.56(8), Pb 44.76(25), Bi 0.26(7), Sb 24.71(11), As 5.33(9), S 20.47(11), total 100.10(39), and 2) Sb-poor sterryite: Cu 0.73(4), Ag 4.12(13), Pb 44.58(16), Sb 20.84(22), As 8.27(12), S 20.92(7), total 99.47(15). The unit cell of Sb-rich sterryite is: a 8.1891(1), b 28.5294(13), c 42.98(2) Å,

§ *E-mail address*: Yves.Moelo@cnrs-imn.fr

† Dedicated to the memory of John L. Jambor (1936–2008)

β 94.896(8)°, V = 10005(5) Å^3 (space group $P2_1/n$). It presents a powder diagram close to that of sterryite from Madoc, Ontario, the type locality. The crystal structures of sterryite and parasterryite (not described here) are very similar, and represent a limiting case of homeotypy; they are also expanded homologues of owyheeite. The structural formula of parasterryite is based on 48 cations and 58 S, ideally $Ag_4Pb_{20}(Sb_{14.5}As_{9.5})_{\Sigma 24}S_{58}$ (Z = 4). The structural formula of sterryite is based on 47 cations and 56 S, with an $(As–As)^{4+}$ dimer [d(As–As) = 2.64 Å] and a specific Cu site, ideally $Cu(Ag,Cu)_3Pb_{19}(Sb,As)_{22}(As–As)S_{56}$ (Z = 4). The presence of the As–As dimer in sterryite indicates its formation with a lower $f(S_2)$ than parasterryite, which may also explain the formation of some rare Pb–Sb–As sulfosalts at Madoc.

Keywords: parasterryite, new mineral species, sterryite, sulfosalt, silver, lead, antimony, arsenic, Pollone mine, Apuan Alps, Tuscany, Italy.

Sommaire

La parasterryite, nouvelle espèce minérale, a été découverte dans le gisement à barite – pyrite – (Pb–Zn–Ag) de Pollone, à Valdicastello Carducci, près de Pietrasanta, Alpes Apuanes, en Toscane, Italie. Elle se présente en cristaux aciculaires (jusqu'à 4 × 0.3 mm) dans des géodes de quartz et barite. La sterryite (second indice mondial) est également présente. Les autres sulfures et sulfosels associés sont la pyrite, la sphalérite, ainsi que des sulfosels variés de Sb,As. La parasterryite est noire à éclat métallique; sous le microscope, elle paraît blanche avec un faible pléochroïsme. L'anisotropie est distincte, avec des teintes verdâtre à brunâtre. Les réflectances minimales et maximales pour les longueurs d'onde de la COM sont [λ (nm), R_{air}, R_{oil} (%)]: 470: 35.1, 40.8 et 19.4, 22.2, 546: 33.5, 39.3 et 19.3, 21.7, 589: 32.7, 38.2 et 18.7, 21.1, 650: 31.4, 36.5 et 17.3, 19.5. Dureté VHN_{10} = 238 kg/mm^2. Les analyses à la microsonde donnent (pds. %, moyenne de 32 anal.): Cu 0.09(3), Ag 4.37(12), Hg 0.15(4), Pb 46.99(45), Sb 19.60(42), As 7.70(28), S 20.57(0.12), total 99.48(49). L'étude aux rayons X sur monocristal indique une symétrie monoclinique, groupe spatial $P2_1/c$, avec a 8.3965(5), b 27.9540(4), c 43.8840(13) Å, β 90.061(12)°, V = 10300(3) Å^3. Les raies principales du diagramme de poudre [d en Å(I)(hkl)] sont: 3.62(100)(075, 01$\underline{1}$2, 234, $\overline{2}3\underline{4}$), 3.42(45)(244, $\overline{2}\underline{4}4$), 3.35(95)(01$\underline{1}\underline{3}$), 3.23(65)(078), 3.01(45)(239 ,$\overline{2}\underline{3}$9), 2.945(85)(088), 2.885(80), 1.916(45). Le nom de parasterryite témoigne de son étroite parenté structurale avec la sterryite. La sterryite est plus abondante que la parasterryite. L'analyse à la microsonde de deux échantillons donne: 1) sterryite riche en Sb (pds. %): Cu 1.27(1), Ag 2.19(11), Hg 0.55(5), Tl 0.56(8), Pb 44.76(25), Bi 0.26(7), Sb 24.71(11), As 5.33(9), S 20.47(11), total 100.10(39); 2) sterryite pauvre en Sb: Cu 0.73(4), Ag 4.12(13), Pb 44.58(16), Sb 20.84(22), As 8.27(12), S 20.92(7), total 99.47(15). La maille élémentaire de la variété riche en Sb (groupe spatial $P2_1/n$) est: a 8.1891(1), b 28.5294(13), c 42.98(2) Å, β 94.896(8)°, V = 10005(5) Å^3. Son diagramme de poudre aux rayons X est proche de celui de la sterryite du gisement-type de Madoc. D'après leurs structures cristallines (non détaillées), la sterryite et la parasterryite sont très semblables, et représentent un cas limite d'homéotypie; ce sont de plus des homologues par expansion de l'owyheeïte. La formule structurale de la parasterryite est fondée sur 48 cations et 58 S, idéalement $Ag_4Pb_{20}(Sb_{14.5}As_{9.5})_{\Sigma 24}S_{58}$ (Z = 4). La formule structurale de la sterryite est fondée sur 47 cations et 56 S, avec un dimère $(As–As)^{4+}$ [d(As–As) = 2.64 Å] et un site spécifique à Cu, idéalement $Cu(Ag,Cu)_3Pb_{19}(Sb,As)_{22}(As–As)S_{56}$ (Z = 4). La présence du dimère As–As dans la sterryite indique une formation à plus basse $f(S_2)$ que la parasterryite, ce qui peut expliquer également la formation d'autres sulfosels rares de Pb–Sb–As à Madoc, Ontario, le gisement-type de la sterryite.

Mots-clés: parasterryite, nouvelle espèce minérale, sterryite, sulfosel, argent, plomb, antimoine, arsenic, gisement de Pollone, Alpes Apuanes, Toscane, Italie.

Introduction

The Pollone mine (latitude 43°57' N, longitude 10°16' E), located at Valdicastello Carducci, near Pietrasanta, in the Apuan Alps, Tuscany, Italy, is a small barite–pyrite deposit. Minor amounts of Pb, Zn, Sb, Ag, As and Cu lead to the formation of various sulfides and sulfosalts, among which the famous geocronite crystals (Kerndt 1845, D'Achiardi 1902). During a routine check of mineral samples (P.O.), acicular crystals of sterryite (second world occurrence) were identified, and this find led to a crystal-structure study. This study permitted us to distinguish some crystals with a unit cell close to but distinct from that of sterryite, corresponding to a distinct compound, which is named *parasterryite* (the Greek prefix *para* meaning "near"). The mineral and the name were approved by the CNMNC–IMA, number 2010–033. The holotype specimens of parasterryite are deposited in the mineralogical collection of Museo di Storia Naturale e del Territorio, Università di Pisa, via Roma 79, Calci (PI), Italy, with catalogue number 19347, and at the Museum of Mineralogy, Ecole des Mines de Paris, with catalogue number 82522.

In this study, we present a mineralogical description of parasterryite and the associated sterryite. Owing to their complexity and their relationship with owyheeite and other Pb–Sb sulfosalts, their crystal structures will be discussed in a separate paper (Moëlo *et al.*, in prep.).

Geological Setting

The Pollone barite – pyrite – (Pb–Zn–Ag) deposit lies in the southern portion of the Sant'Anna tectonic window (Fig. 1), where metamorphic rocks outcrop surrounded by the non-metamorphic sedimentary formations of the Tuscan Nappe. The deposit is hosted in the Scisti di Fornovolasco Formation, belonging to the Fornovolasco–Panie Unit. According to Ciarapica

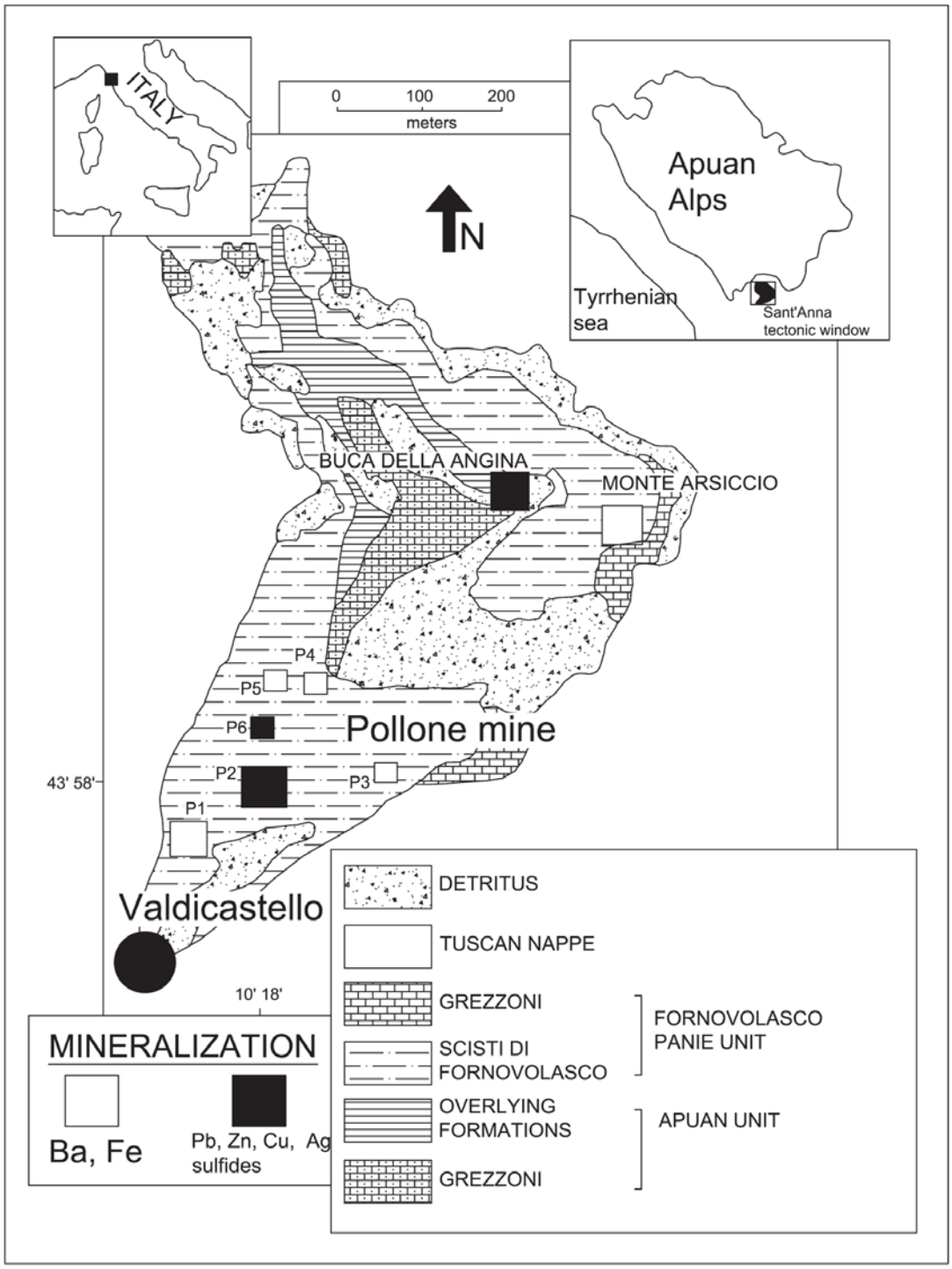

FIG. 1. Geological map of the Sant'Anna tectonic window, showing the most important mineral deposits: the Pollone barite – pyrite – (Pb–Zn–Ag) deposit (P1 to P6 outcrops), the Cu(Au) vein system of Buca dell'Angina, and the Monte Arsiccio barite – pyrite – iron oxides deposit (modified from Costagliola *et al*. 1998).

et al. (1985), this unit consists of the Stazzema slices and the Panie Unit; in particular, the Stazzema slices are a complicated pile of Paleozoic rocks, "Grezzoni" and "Pseudomacigno", and in the Sant'Anna tectonic window, they overlie the so-called Apuan Unit, formed by the lowermost portion of the metamorphic complex of the Apuan Alps.

The polymetamorphic basements of both these tectonic units show many similarities; in fact, they are predominantly formed by siliciclastic and metavolcanic rocks of Paleozoic age. Recently, Pandeli *et al*. (2004) correlated the Scisti di Fornovolasco Formation with the Variscan basement of the Apuan Unit. These rocks were metamorphosed to the greenschist facies during the Alpine events. According to Carmignani & Kligfield (1990), two major phases of deformation affected the area: a compressional phase (D_1), dated at 27 Ma, followed by an extensional phase (D_2) at 12–8 Ma (Kligfield *et al*. 1986). During the D_2 phase, several shear zones developed, in response to the gravitational collapse of the Apuan Alps core complex, as proposed by Carmignani & Kligfield (1990).

Together with the Monte Arsiccio and Buca della Vena mines, the Pollone deposit occurs in a barite district that has been extensively studied (Lattanzi *et al*. 1994, and references therein). According to Costagliola *et al*. (1998), vein formation at Pollone was controlled by the development of shear zones during the D_2 phase; mineralized bodies were emplaced in response to syndeformation and synmetamorphic circulation of fluids, which was focused along the shear zone affecting the northern sector of the deposit. Estimates of P–T indicate that host and country rocks record metamorphic temperatures of about 350°C, on the basis of chlorite and arsenopyrite geothermometers; the phengite geobarometer, for a T value of 350°C, shows a frequency peak around 0.35 GPa. Appreciably higher temperatures (around 450°C) were found for the mineralizing fluids; such a difference of temperature could reflect a thermal disequilibrium between rocks and fluids, suggesting that the latter were not produced locally but came from a higher temperature, and possibly deeper, reservoir than the Pollone rocks (Costagliola *et al*. 1998).

The Pollone deposit belongs to the same type of barite, pyrite, and iron oxides deposits as the Buca della Vena (Benvenuti *et al*. 1986, Orlandi & Dini 2004), Canale delle Radice (Carmignani *et al*. 1976), Monte Arsiccio (Costagliola *et al*. 1990) and Fornovolasco (Biagioni *et al*. 2008, Orlandi *et al*. 2008) deposits; all these ore deposits are characterized by the occurrence of acicular sulfosalts of lead as accessory minerals.

Occurrence and Mineralogical Association

The Pollone mine was exploited in the Middle Ages for argentiferous galena; only in the 20th century was the mining activity focused on barite exploitation. The first mineralogical study was performed on samples from this locality by Kerndt (1845), who described the geocronite crystals; the presence of Ag sulfosalts was first reported by Carmignani *et al*. (1975, 1976), who cited the presence of argentiferous tetrahedrite and owyheeite. Brizzi & Olmi (1989) described the occurrence there of proustite, and Frizzo & Simone (1995) observed the presence of diaphorite as exsolution blebs and intergrowths in galena from the Preziosa tunnel.

Parasterryite and sterryite were collected independently in vugs within barite–quartz veins embedded in barite–pyrite lenses. An overgrowth of minute yellow-green crystals of sphalerite was observed on the sterryite needles, whereas parasterryite is free of any sulfide or sulfosalt. During this study, acanthite, famatinite, geocronite–jordanite, pyrargyrite–proustite, Sb-rich rathite, tetrahedrite and xanthoconite were also identified in the same occurrence. Owyheeite and a boulangerite-like sulfosalt described by Carmignani *et al*. (1975) were found in this kind of occurrence, but they were not identified in the samples studied. Boulangerite was identified in quartz veins embedded in the country rocks, as acicular to prismatic crystals, up to several cm in length.

Parasterryite

Mineral description

Parasterryite occurs as metallic black needles striated along their elongation (**a** axis); they attain up to several mm in length and are 0.2 to 0.3 mm thick (Fig. 2). It is brittle, with a conchoidal fracture, and there seems to be a poor cleavage perpendicular to the elongation (Fig. 2); the streak is black. Under the microscope, it appears white, without internal reflections. Pleochroism is weak, from greyish white to white, more distinct in oil. This corresponds to a distinct bireflectance. With crossed polars, anisotropism is distinct in air, strong in oil, with rotation tints varying from gray to dark gray, with brownish and greenish tints. Extinction is oblique (20–30°), and a lamellar twinning is present parallel to the elongation. Strong striations of the needles (Fig. 2) confirm such a polysynthetic twinning.

The reflectance has been measured in air and oil (n = 1.515) on a section parallel to the elongation, with WTiC as a standard. Table 1 gives the reflectance values, and Figure 3 shows the two pairs of reflectance curves. These curves slightly decrease with increasing wavelength; they are similar to optical data obtained for complex Pb–Sb sulfosalts discovered in the neighboring Ba–Fe deposit of Buca della Vena, such as scainiite, pillaite and pellouxite (Orlandi *et al*. 1999, 2001, 2004).

The Vickers hardness was difficult to determine because of the small size of the crystals. Only three indentations (two with a load of 25 and one with a load of 10 g) were obtained. The VHN_{25} is 196, and VHN_{10}, 238 kg/mm^2. These values correspond to a Mohs hardness close to 4, which probably is too high. A value

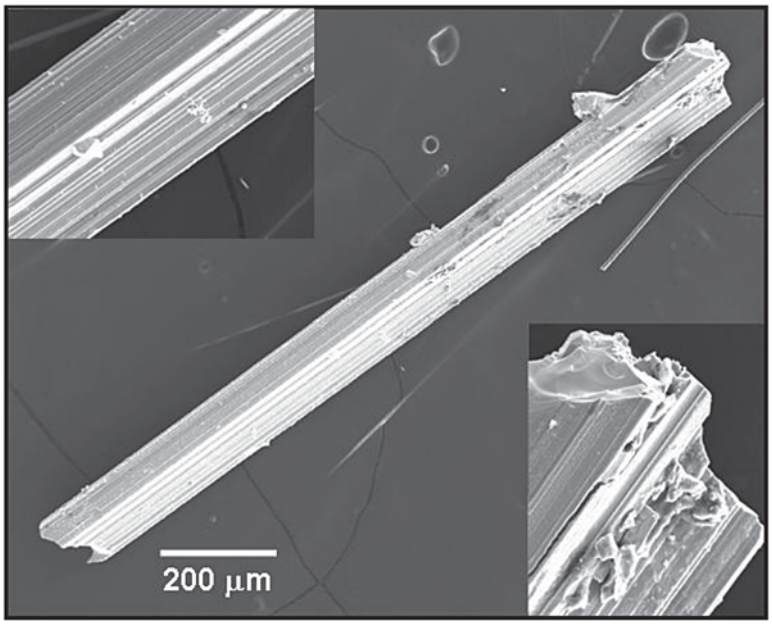

FIG. 2. SEM image (back-scattered electron image) of a parasterryite needle. Upper left: detail of the striations due to polysynthetic twinning; lower right: broken termination, with a conchoidal fracture, and probably a poor cleavage perpendicular to the elongation.

TABLE 1. REFLECTANCE DATA FOR PARASTERRYITE IN AIR AND OIL

	in air		in oil	
λ (nm)	R_{min}	R_{max}	R_{min}	R_{max}
400	32.6	37.8	19.8	20.5
420	35.0	40.2	18.0	21.1
440	34.5	40.2	18.9	21.6
460	35.1	40.9	19.3	22.1
470	**35.1**	**40.8**	**19.4**	**22.2**
480	34.8	40.8	19.6	22.3
500	34.3	40.1	19.5	22.1
520	33.6	39.7	19.5	22.0
540	33.7	39.6	19.4	21.8
546	**33.5**	**39.3**	**19.3**	**21.7**
560	33.3	39.0	19.0	21.6
580	32.9	38.7	18.8	21.5
589	**32.7**	**38.2**	**18.7**	**21.1**
600	32.5	38.0	18.3	20.9
620	32.3	37.5	18.0	20.4
640	31.6	36.4	17.5	19.8
650	**31.4**	**36.5**	**17.3**	**19.5**
660	31.3	36.3	17.0	19.3
680	30.8	35.4	16.3	18.5
700	30.4	34.6	16.1	18.2

between 3 and 3½ is more realistic. The density could not be measured because of the scarcity of the material. The calculated density, on the basis of the ideal formula $Ag_4Pb_{20}(Sb_{14.5}As_{9.5})_{\Sigma 24}S_{58}$, is 5.747 g/cm^3.

Chemical composition

An electron-microprobe analysis was carried out with a Camebax SX50 apparatus (BRGM–CNRS–University common laboratory, Orléans, France) at 20 kV and 20 nA. Following standards were used [element, emission line, counting time (s)]: pyrite (S*K*α, 20), Cu metal (Cu*K*α, 30), stibnite (Sb*L*α, 20), Ag metal (Ag*L*α, 20), AsGa (As*L*α, 30), galena (Pb*M*α, 20), lorandite (Tl*M*α, 20), Bi element (Bi*M*α, 20), and cinnabar (Hg*M*α, 20). Some other elements were sought, but not detected (detection limit, wt.%): Cl (0.02), Sn and Cd (0.12), Se (0.04) and Fe (0.05).

Results of the analysis of parasterryite are given in Table 2. To enhance the accuracy of this analysis and document its distinction from sterryite, we carried out a set of 32 spot analyses that indicate a very good wt.% total [from 98.63 up to 100.42, with a mean 99.48(49) wt.%], as well as a good charge-balance [relative error on the valence equilibrium *Ev* from –1.1 up to 1.9%, mean 0.5(0.8)]. Parasterryite contains four major cations: Pb, Sb, As and Ag, with traces of Cu and Hg [mean 0.13(4) and 0.07(2) wt.%, respectively].

Crystallography

The unit cell of parasterryite (Table 3) has been established in our crystal-structure study using a Nonius

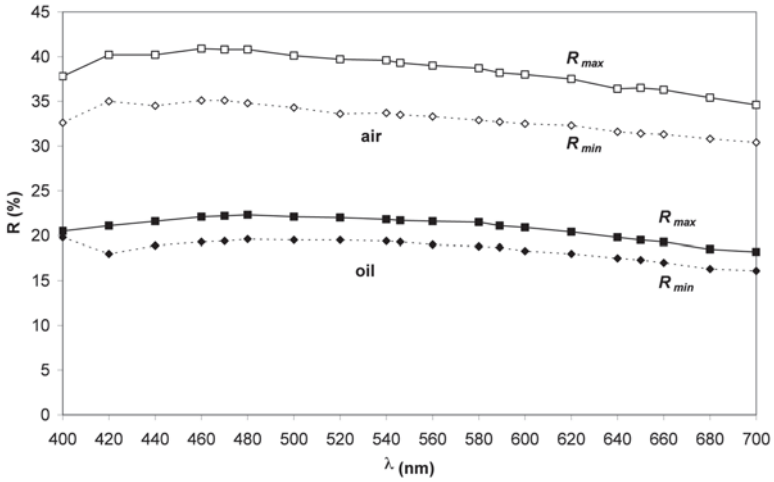

FIG. 3. Reflectance curves of parasterryite in air and oil.

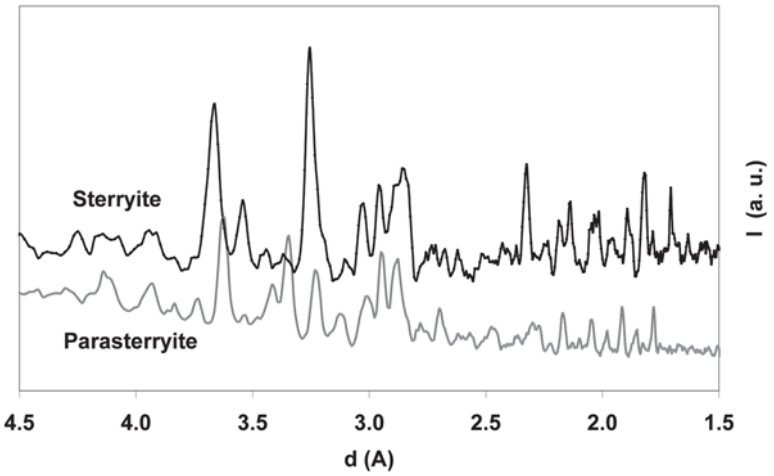

FIG. 4. Comparison of X-ray powder spectra of Sb-rich sterryite (upper) and parasterryite (down) in the *d* range 1.5–4.5 Å.

Kappa CCD detector. Parasterryite is monoclinic $P2_1/c$, with a pseudo-orthorhombic symmetry [$\beta = 90.06(1)°$]. The unit-cell volume is significantly greater than that of sterryite (by about 3%); nevertheless, its *b* parameter is 2% lower than that of Sb-rich sterryite.

Figure 4 presents the powder-diffraction spectrum obtained on a single-crystal fragment, compared with that of sterryite. Although similar in the general distribution and intensities of diffraction lines, these spectra are significantly different, and permit us to distinguish univocally the two species. Table 4 gives the measured powder-diffraction pattern of parasterryite, compared to the calculated one on the basis of the crystal-structure study. One can see that there are generally several calculated diffraction-lines for each measured one, which did not permit us to refine the unit cell of parasterryite on the sole basis of the XRPD spectrum.

The single-crystal study also led us to document the presence of twinning, with (001) as the twin plane.

STERRYITE

Mineral description

Sterryite and parasterryite cannot be distinguished qualitatively under the binocular or the microscope. Sterryite, more common than parasterryite, occurs as lead-grey prismatic crystals, elongate and striated on [100], usually up to a few mm long, but exceptionally up to 3 cm. Crystals are usually included in quartz or barite; in some cases, it is possible to find crystals protruding inside small vugs of the barite matrix. Sterryite is generally superficially altered to earthy black products.

In the polished section used for the electron-microprobe analysis, small areas closely associated to a large crystal of sterryite correspond to famatinite, Cu_3SbS_4, according to the microprobe results; the mean of three spot analyses, in wt.%, is Sb 27.3, Cu 39.6, Pb 1.0, As 0.6, Ag 0.8, S 28.0, Cl 0.1, sum 97.4, and the unit formula (on the basis of S + Cl = 4 *apfu*) is $Cu_{2.85}Ag_{0.03}Sb_{1.03}As_{0.03}Pb_{0.02}S_{3.99}Cl_{0.01}$. The formation of famatinite, formally $Cu^{+}{}_3Sb^{5+}S^{2-}{}_4$, implies a high $f(S_2)$, whereas that of sterryite relates to a low $f(S_2)$ (see Discussion); this indicates non-equilibrium conditions (probably two distinct stages in the mineral succession).

Chemical composition

Table 5 gives two sets of electron-microprobe results, corresponding to Sb-rich and Sb-poor varieties of sterryite. They contain the major cations Pb, Sb and As, together with minor Ag and Cu. The Sb-rich variety also contains significant amounts of Hg, Tl and Bi. The analytical totals are good, but calculated *Ev* indicates an excess of positive charges [means 2.4(3) and 1.5(7)%, respectively] relative to parasterryite (see explanation below).

TABLE 2. THE COMPOSITION OF PARASTERRYITE

	Mean	Max.	Min.	σ	Ideal *
Cu wt.%	0.09	0.11	0.06	0.02	
Ag	4.36	4.43	4.22	0.06	4.84
Hg	0.15	0.18	0.12	0.02	
Pb	47.00	47.32	46.83	0.18	46.49
Sb	19.57	19.80	19.25	0.30	19.81
As	7.73	8.18	7.59	0.21	7.99
S	20.56	20.65	20.48	0.07	20.87
Sum	99.46	99.77	99.20	0.23	100
Cu *apfu*	0.13	0.15	0.09	0.04	
Ag	3.65	3.69	3.54	0.10	4
Hg	0.07	0.08	0.06	0.02	
Pb	20.41	20.47	20.34	0.14	20
Sb	14.49	14.62	13.93	0.33	14.5
As	9.25	9.78	9.12	0.32	9.5
S	57.72	58.10	57.46	0.46	58
Ev **	0.5	0.8	-0.1	0.2	0
Cu+Ag+Hg	3.83	3.90	3.74	0.05	4
Sb + As	23.74	23.79	23.64	0.05	24
As/(As+Sb)	0.391	0.412	0.385	0.010	0.417
Pb/(Sb+As)	0.859	0.866	0.855	0.004	0.833

Electron-microprobe data (sample no. 4960, mean result of 32 spot analyses). The atomic proportions are calculated on the basis of a cation total of 48 atoms. * Ideal: $Ag_4Pb_{20}(Sb_{14.5}As_{9.5})_{\Sigma 24}S_{58}$; ** Ev: relative error (%) on the valence equilibrium. Detection limits (wt.%): Cu 0.05; Ag 0.12.

Crystallography

An X-ray single-crystal study of sterryite with a Nonius Kappa CCD gave a monoclinic unit-cell, corresponding to the true ~8 Å structure observed by Jambor (1967b) at the type locality in Madoc, Ontario, whereas this author gave an orthorhombic symmetry for the observed ~4 Å substructure (Table 3). The higher unit-cell volume of the Pollone sterryite is due to its higher Sb/As value.

In Table 6, we give the XRPD diagram of Sb-rich sterryite, compared to that of sterryite from Madoc, and to the calculated pattern derived from the crystal structure. Figure 4 shows this pattern compared to that of parasterryite. According to the crystal structures, the *a* periodicity is quite identical to d_{100} in parasterryite and close to $2d_{\bar{2}01}$ in sterryite, as illustrated by the values of the two diffraction lines d_{400} of parasterryite [Table 4: d_{400} (meas.) = 2.098 Å, that is d_{100} = 8.392 Å, close to a = 8.397 Å] and $d_{\bar{4}02}$ of sterryite [Table 6: $d_{\bar{4}02}$ (meas.) = 2.049 Å ($d_{calc.}$ = 2.0472 Å), that is $d_{\bar{4}02}$ = 8.196 Å, close to a = 8.189 Å].

Twinning according to the same twin law [twin plane (001)] as for parasterryite was confirmed in this X-ray study.

COMPARATIVE CRYSTAL CHEMISTRY OF STERRYITE AND PARASTERRYITE

Structural formulas

A full comparison of the structures of sterryite and parasterryite will be presented in a separate paper

TABLE 3. UNIT CELLS OF PARASTERRYITE AND STERRYITE

a (Å)	*b* (Å)	*c* (Å)	β (°)	Space group	*V* (Å^3)	δ*V*
Sterryite, Madoc, Ontario*						
28.4	42.6	8.26		*Pba*2 or *Pbam*	9921	
Sb-rich sterryite, Pollone, Italy						
8.1891	28.5294)	42.98	94.896	$P2_1/n$	10005	0.8
0.0001	0.0013	0.02	0.008		5	
Parasterryite, Pollone, Italy						
8.3965	27.9540	43.8840	90.061	$P2_1/c$	10300	3.8
0.0005	0.0004	0.0013	0.012		3	

* Jambor (1967b). δ*V* is expressed in %.

TABLE 4. OBSERVED AND CALCULATED X-RAY POWDER-DIFFRACTION DATA FOR PARASTERRYITE

I_{meas}	d_{meas}	d_{calc}	I_{calc}	h k l	I_{meas}	d_{meas}	d_{calc}	I_{calc}	h k l
		5.518	5	$\bar{1}$ 0 6	15	2.569B	2.568	5	2 8 5
15	5.45	5.512	6	1 0 6			2.568	5	2 5 11
20	4.71	4.715	25	0 5 5	20	2.462B	2.462	11	$\bar{2}$ $\bar{9}$ 3
10	4.30	4.315	13	0 4 8			2.461	10	2 9 3
		4.288	7	0 6 4	15	2.362B	2.367	5	$\bar{2}$ 2 15
		4.152	56	2 1 0			2.298	10	$\bar{2}$ $\bar{10}$ 3
35	4.14B	4.134	21	$\bar{2}$ $\bar{1}$ 1	15	2.299B	2.298	11	2 10 3
		4.133	10	2 1 1			2.292	5	$\bar{2}$ 6 13
		4.115	19	0 6 5			2.276	5	$\bar{2}$ $\bar{10}$ 4
		3.949	20	0 1 11	25	2.269	2.276	6	2 10 4
40	3.94B	3.930	14	0 6 6			2.265	5	2 2 16
		3.929	9	0 7 2	10	2.221	unindexed (impurity?)		
10	3.84	3.828	5	2 3 0			2.171	14	$\bar{2}$ $\bar{11}$ 1
20	3.73	3.739	33	0 6 7			2.171	20	2 $\bar{11}$ 1
		3.635	87	0 7 5	35	2.170	2.164	8	$\bar{2}$ $\bar{11}$ 2
100	**3.62**	3.626	23	0 1 12			2.163	9	2 11 2
		3.615	13	$\bar{2}$ $\bar{3}$ 4			2.158	17	0 8 16
		3.613	19	2 3 4			2.099	79	4 0 0
5	3.54	3.551	23	0 6 8	10	2.098	2.099	8	$\bar{2}$ 4 17
		3.522	7	2 2 6			2.097	10	2 4 17
45	**3.42**	3.420	49	$\bar{2}$ $\bar{4}$ 4			2.047	16	$\bar{2}$ 5 17
		3.419	45	2 4 4	30	2.045	2.046	12	2 5 17
95	**3.35**	3.351	100	0 1 13			2.043	20	0 5 20
		3.246	27	0 8 5			1.9853	10	0 9 17
65	**3.23**	3.229	49	0 7 8	20	1.979B	1.9784	11	0 14 3
		3.122	9	$\bar{2}$ $\bar{4}$ 7			1.9200	6	2 6 18
		3.120	9	2 4 7			1.9139	16	2 13 0
30	3.12B	3.115	9	0 1 14	**45**	**1.916**	1.9121	10	$\bar{2}$ $\bar{13}$ 1
		3.111	5	$\bar{2}$ $\bar{6}$ 1			1.9120	10	2 13 1
		3.111	7	2 6 1			1.8568	5	$\bar{2}$ 6 19
		3.012	36	$\bar{2}$ $\bar{3}$ 9	25	1.851	1.8554	9	2 6 19
45	**3.01B**	3.009	37	2 3 9			1.8536	17	0 13 12
		2.989	5	0 9 4			1.8487	5	0 15 3
85	**2.945**	2.947	72	0 8 8			1.8309	5	$\bar{4}$ $\bar{6}$ 7
		2.894	14	2 7 0			1.8299	6	4 6 7
		2.886	14	$\bar{2}$ $\bar{3}$ 10	10	1.828B	1.8285	9	0 0 24
80	**2.885B**	2.883	24	2 3 10			1.8181	7	$\bar{4}$ $\bar{7}$ 5
		2.878	18	$\bar{2}$ 1 11			1.8175	7	$\bar{4}$ $\bar{1}$ 12
		2.875	14	2 1 11			1.8174	13	4 7 5
		2.868	9	2 7 2			1.7799	24	$\bar{2}$ 12 12
		2.784	5	$\bar{2}$ $\bar{4}$ 10	40	1.779	1.7798	14	$\bar{4}$ $\bar{1}$ 13
15	2.780	2.783	5	0 9 7			1.7791	21	2 12 12
		2.782	13	2 4 10			1.7781	13	4 1 13
		2.704	11	2 2 12	10	1.505			
30	2.670B	2.703	28	0 9 8	15	1.473			
		2.681	5	$\bar{2}$ $\bar{8}$ 1	15	1.442			
		2.681	9	2 8 1	15	1.390			
10	2.621	2.628	9	$\bar{2}$ $\bar{7}$ 7	10	1.366			

Bold-face font: main powder-diffraction lines.

(Moëlo *et al.*, in prep.). The two structures are based on a single building block, corresponding to a complex column with a pseudotrigonal core and two "arms" (= ribbon projections) of unequal lengths (Fig. 5). These structures are topologically very similar, and differ essentially in the configuration and composition of the shorter arm (Fig. 5: lozenge A for sterryite, and lozenge B for parasterryite). Ribbon A of sterryite presents a tetrahedral Cu site, and an As–As pair subparallel to the **a** axis; the short bond that characterizes this pair has d(As–As) = 2.64 Å, close to d(As–As) = 2.57 Å of the As–As pair in the crystal structure of realgar (Mullen & Nowacki 1972); the composition of ribbon A is approximately $CuSb_2Pb(Pb,Sb)(As–As)S_8$ (= Me_7S_8). Ribbon B of parasterryite is a little bit longer, with composition $Ag_2(Pb,As)Sb(Sb,As)As_3S_{10}$ (= Me_8S_{10}); this explains the significant increase in the *c* parameter.

Thus the unit formula of parasterryite ($Me_{48}S_{58}$) contains one *Me* and two S atoms in excess of that in sterryite ($Me_{47}S_{56}$), which is the reason for the increase in the unit-cell volume. The small decrease in *b* (–2%) is related principally to its greater As/(Sb+As) atomic ratio: 0.39 (Table 2b) *versus* 0.26 for Sb-rich sterryite (Table 5b). The *a:b:c* proportions of parasterryite

are 0.300:1:1.570, whereas those of Sb-rich sterryite are 0.287:1:1.507 [sterryite from Madoc (Table 3): 0.291:1:1.500].

On the basis of *Me* = 47 atoms, the electron-microprobe data for Sb-rich sterryite (Table 2) give: $Cu_{1.75(1)}Ag_{1.78(9)}Hg_{0.24(2)}Tl_{0.24(4)}Pb_{18.90(7)}Bi_{0.11(3)}Sb_{17.76(7)}As_{6.23(11)}S_{55.85(12)}$, and for the Sb-poor variety: $Cu_{0.98(5)}Ag_{3.29(10)}Pb_{18.51(10)}Sb_{14.72(13)}As_{9.50(13)}S_{56.13(36)}$. Owing to their low content, Hg, Tl and Bi of the Sb-rich variety could not be precisely located in the structure; Hg probably substitutes at some Ag positions. Without these minor cations, the ideal formula is: $Cu(Ag,Cu)_3Pb_{19}(Sb_{18-15}As_{4-7})_{\Sigma 22}(As–As)S_{56}$ ($Z = 4$). The presence of an $(As–As)^{4+}$ pair neutralizes two positives charges, which must be substracted for the calculation of *Ev*. The resulting corrected values $Ev_{cor.}$ are 0.4(3) and –0.5(7)% for Sb-rich and Sb-poor varieties, respectively, now respecting the valence equilibrium.

On the basis of 48 *Me* atoms, the electron-microprobe data for parasterryite (Table 2) give: $Cu_{0.13(4)}Ag_{3.65(10)}Hg_{0.07(2)}Pb_{20.41(14)}Sb_{14.49(33)}As_{9.25(32)}S_{57.72(66)}$. The ideal formula is: $Ag_4Pb_{20}(Sb_{14.5}As_{9.5})_{\Sigma\ 24}S_{58}$ ($Z = 4$). Parasterryite has roughly the same As/(As+Sb) value as Sb-poor sterryite, but presents a significantly higher Pb/(Bi+Sb+As) value than sterryite [0.86(1) *versus* 0.78(1) and 0.76(1) for Sb-rich and Sb-poor varieties].

Homeotypy between sterryite and parasterryite

Despite the significant differences between their structural formulas, principally due to the short arm of their constitutive building block, sterryite and parasterryite have very close unit-cells, with monoclinic symmetry but distinct space-groups. Parasterryite is pseudo-orthorhombic ($\beta = 90.061°$), and the orthorhombic subcell of sterryite noted by Jambor (1967b) corresponds to the subcell derived from the monoclinic cell according to $\mathbf{a}' = \mathbf{a}/2$, $\mathbf{b}' = \mathbf{b}$, $\mathbf{c}' = \mathbf{c} + \mathbf{a}/2$, and $\beta' = 90.570°$. This pseudo-orthorhombic symmetry explains the twinning with (001) as the twin plane for the two species.

This strong crystallographic relationship between sterryite and parasterryite allows us to consider this sulfosalt pair as a limiting case of homeotypy. Chemical differences as well as distinct space-groups preclude a solid solution between these two species, but epitactic or syntactic intergrowths are quite possible.

Comparison with sterryite from Madoc

Sterryite was defined from the material collected at Madoc, Ontario (Jambor 1967b). Table 3 compares its unit-cell parameters with those of Sb-rich sterryite and

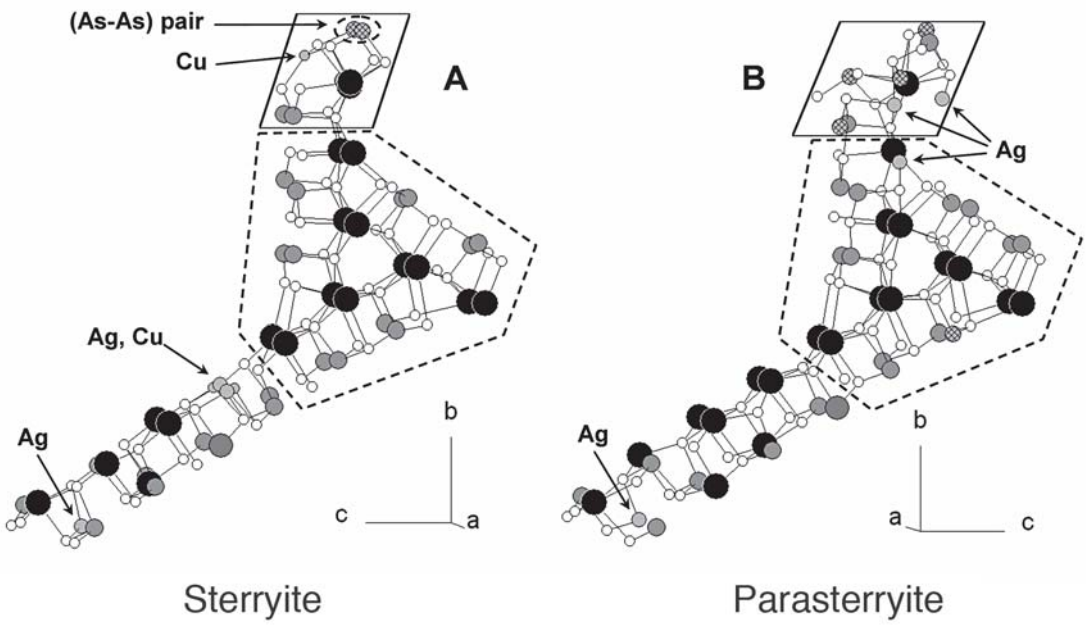

FIG. 5. Projections parallel to the elongation of the building blocks of Sb-rich sterryite and parasterryite. The central triangular column mimicking the owyheeite motif is outlined by a broken line. A and B lozenges represent the distinctive ribbons of each species. Atoms in decreasing size: Pb (black), Sb and (Sb,As) (dark grey), As (dark grey, cross-hatched), Ag (light grey), Cu (light grey), and S (white).

parasterryite from Pollone. Its unit-cell volume is close to that of Sb-rich sterryite.

The chemical composition of the type samples of sterryite was re-examined by Jambor *et al.* (1982) and Moëlo (1983). In Table 7, we compare these results with mean compositions of sterryite and parasterryite from Pollone. Sterryite from Madoc has a Cu content close to that of the Sb-poor variety from Pollone, with an intermediate As/(As+Sb) value between Sb-rich and Sb-poor varieties. But Jambor *et al.* (1982) also indicated a large variation in this ratio (Sb from 20.5 up to 26.6 wt.%, together with As from 8.3 down to 2.9 wt.%).

Comparison with owyheeite

According to the crystal-structure study (Moëlo *et al.*, in prep.), sterryite and parasterryite are expanded derivatives of owyheeite, as their building blocks include the building block of owyheeite, according to Laufek *et al.* 2007 (Fig. 5). As pointed out initially by Moëlo (1983), this structural derivation results in two similar parameters close to 8.2 and 28 Å, whereas the third parameter increases from about 23 Å up to 43–44 Å. Such an expansion of only one parameter allows us to define sterryite and parasterryite as complex homologous derivatives of owyheeite. All these three sulfosalts have a crystal structure built around a pseudotrigonal core, which relates them to the zinkenite plesiotypic series (sulfosalts of the cyclic rod-type and derivatives: Makovicky 1985, Moëlo *et al.* 2008).

Contrary to sterryite and parasterryite, electron-microprobe analyses of owyheeite (Moëlo *et al.* 1984) indicate only minor amounts of arsenic. Its highest content (~1.8 wt.%, Table 7) has been documented in owyheeite from the Pollone mine (Carmignani *et al.* 1976). Copper, where present, is significantly below the Cu content of sterryite (maximum 0.45 wt.%: Moëlo *et al.* 1984).

TABLE 5. COMPOSITION OF STERRYITE FROM THE POLLONE MINE

	Sb-rich		Sb-poor	
	Mean (4)	σ	Mean (7)	σ
Cu wt.%	1.27	0.01	0.73	0.04
Ag	2.19	0.11	4.12	0.13
Hg	0.55	0.05	-	-
Tl	0.56	0.08	-	-
Pb	44.76	0.25	44.58	0.16
Bi	0.26	0.07	-	-
Sb	24.71	0.11	20.84	0.22
As	5.33	0.09	8.27	0.12
S	20.47	0.11	20.92	0.07
Sum	100.10	0.39	99.47	0.15
Cu *apfu*	1.75	0.01	0.98	0.05
Ag	1.78	0.09	3.29	0.10
Hg	0.24	0.02	-	-
Tl	0.24	0.04	-	-
Pb	18.90	0.07	18.51	0.10
Bi	0.11	0.03	-	-
Sb	17.76	0.07	14.72	0.13
As	6.23	0.11	9.50	0.13
S	55.85	0.12	56.13	0.36
Ev	2.4	0.3	1.5	0.7
Ev_{cor}	0.4	"	-0.5	"
Cu+Ag+Hg	3.77	0.06	4.27	0.10
Bi+Sb+As	24.09	0.08	24.2	0.1
As/(As+Sb)	0.260	0.004	0.392	0.005
Pb/(Bi+Sb+As)	0.784	0.006	0.764	0.007

Electron-microprobe data. The atomic proportions are calculated on the basis of a cation total of 47 atoms. Detection limit for Hg, Tl and Bi: 0.15 wt.%. Ev_{cor} = Ev – 2, because of the presence of a $(As–As)^{4+}$ pair.

Distinctions among parasterryite, sterryite, and owyheeite

Parasterryite and sterryite are indistinguishable under the binocular microscope and in reflected light. The simplest way to distinguish them is by chemical analysis with a SEM equipped with energy-dispersion spectrometry, focused on their Ag and Cu contents: parasterryite is quite Cu-free (less than 0.1–0.2 wt.% Cu), whereas sterryite contains from 0.70 up to 1.27 wt.% (Madoc and Pollone, respectively). On the other hand, parasterryite is richer in Ag (about 4.5 wt.%), whereas sterryite contains from 2.3 up to 3.7 wt.% (Pollone and Madoc, respectively: Table 7). Owyheeite, also present at Pollone (Carmignani *et al.* 1976), has a similar acicular habit, and can be distinguished by its low As content (~1.8 wt.%), its higher Ag content (5–6 wt.%), and low Cu content (<0.5 wt.%) (Moëlo *et al.* 1984).

Discussion: Geochemistry and Conditions of Formation

The major and minor components of sterryite and parasterryite (Pb, Sb, As, Ag, Cu) are known in other common sulfosalts at Pollone: tetrahedrite, bournonite, geocronite–jordanite, and pyragyrite–proustite. Mercury, detected in parasterryite and Sb-rich sterryite, is present at Pollone as cinnabar (Carmignani *et al.* 1975). In contrast, Tl and Bi, detected in Sb-rich sterryite, have not been encountered up to now as specific sulfides or sulfosalts. Thus, the geochemical complexity of the ore association at Pollone may lead to the discovery of other rare or new sulfosalts.

The existence of an As–As pair in the structure of sterryite is critical for its stabilization. Its presence indicates a sulfur deficit [low $f(S_2)$] in the crystallization medium, as does the formation of S-poor arsenic sulfides also with As–As bonding (realgar and pararealgar, As_4S_4; uzonite, As_4S_5; alacranite, As_8S_9; wakabayashilite, $[(As,Sb)_6S_9][As_4S_5]$ Bonazzi *et al.* 2005). Such a relatively low fugacity of sulfur may also be necessary for the stabilization of other Pb–Sb–As

TABLE 6. X-RAY POWDER-DIFFRACTION DATA FOR Sb-RICH STERRYITE FROM THE POLLONE MINE (THIS STUDY) AND FOR STERRYITE FROM MADOC*

Madoc		Pollone		Structure					Madoc		Pollone		Structure				
d	*I*	*d*	*I*	d_{calc}	I_{calc}	*h*	*k*	*l*	*d*	*I*	*d*	*I*	d_{calc}	I_{calc}	*h*	*k*	*l*
				17.125	38	0	$\bar{1}$	$\bar{2}$	2.913	3			2.913	24	$\bar{2}$	$\bar{5}$	8
				14.265	22	0	2	0					2.912	34	2	2	9
				13.534	47	0	2	1			2.894	13	2.897	11	0	9	6
				12.766	16	0	$\bar{1}$	$\bar{3}$					2.884	31	$\bar{2}$	2	11
11.77	2			11.871	5	0	2	2					2.883	16	2	7	0
10.69	<½			**10.706**	**100**	0	0	$\bar{4}$					2.881	16	$\bar{2}$	$\bar{7}$	2
8.64	<½			8.563	29	0	2	4					2.854	19	0	8	9
8.20	<½			8.203	16	0	$\bar{1}$	$\bar{5}$			**2.855**	**48B**	2.853	31	2	6	5
7.94	<½			7.914	33	0	3	3					2.839	16	2	3	9
				7.137	5	0	0	$\bar{6}$					**2.838**	**44**	$\bar{2}$	$\bar{6}$	7
		7.13	4B	7.126	6	$\bar{1}$	$\bar{1}$	3	**2.836**	**7**	2.832	4	2.835	21	2	0	10
7.11	3			7.110	26	0	3	4					2.813	12	$\bar{2}$	3	11
		7.03	10	7.035	12	0	4	1					2.807	22	$\bar{2}$	0	12
6.38	<½			6.380	8	0	4	3					2.784	11	$\bar{2}$	$\bar{7}$	5
5.96	0.5	6.00	8	6.054	7	$\bar{1}$	$\bar{3}$	2					2.781	22	2	2	10
				5.671	11	1	0	5	2.778	2			2.776	17	2	6	6
		5.63	5	5.656	5	0	5	1					2.759	15	$\bar{2}$	$\bar{6}$	8
				5.366	9	$\bar{1}$	$\bar{4}$	1			2.756	5	2.755	17	$\bar{2}$	2	12
				5.353	8	0	0	$\bar{8}$					2.743	22	2	7	4
5.29	<½			5.270	6	1	2	$\bar{5}$	2.732	3	2.731	8	2.731	17	$\bar{2}$	$\bar{7}$	6
		5.25	3	5.261	7	0	$\bar{1}$	$\bar{8}$					2.728	13	0	9	8
4.98	<½?	5.04	3?								2.715	8	2.717	11	2	3	10
		4.78	3	4.755	5	0	6	0					2.689	15	$\bar{2}$	$\bar{8}$	1
				4.749	32	0	5	5					2.685	7	0	7	12
4.72	1			4.726	9	0	6	1	2.684	2	2.675	12B	2.684	14	2	7	5
		4.71	7	4.693	21	0	$\bar{1}$	$\bar{9}$					2.671	11	$\bar{2}$	$\bar{7}$	7
				4.665	7	0	3	8					2.630	10	0	8	11
				4.511	5	0	6	3	2.622	2	2.621	11	2.619	5	2	7	6
4.50	1	4.50	11	4.500	5	$\bar{1}$	3	7	2.516	<½?	2.518	7B					
4.34	0.5			4.346	13	0	6	4	2.487	<½			2.477	6	2	7	8
				4.282	14	0	0	$\bar{10}$					2.438	5	0	11	6
4.26	2	4.25	10	4.281	12	0	4	8	2.435	0.5	2.428	9	2.435	6	2	6	10
				4.173	8	0	5	7	2.415	0.5			2.417	6	$\bar{2}$	6	12
4.14	5	4.16	8B	4.157	20	0	6	5			2.408	6	2.409	6	2	8	7
		4.12	8B	4.102	29	0	2	10					2.397	6	$\bar{2}$	$\bar{8}$	9
				4.092	8	$\bar{1}$	2	9					2.375	5	0	4	17
4.08	0.5			4.080	16	2	0	0	2.370	0.5	2.369	8	2.374	6	0	12	1
		4.07	8B	4.072	13	$\bar{2}$	0	2	**2.353**	**6**?							
				4.004	11	0	7	2					2.328	18	2	10	1
				3.989	21	2	1	1			**2.324**	**44**	2.325	17	$\bar{2}$	$\bar{10}$	3
				3.975	17	$\bar{2}$	$\bar{1}$	3					2.284	13	2	3	14
				3.958	23	0	4	9	2.260	0.5			2.264	12	$\bar{2}$	3	16
3.94	5	3.94	13B	3.946	9	2	0	2			2.251	5	2.257	5	0	4	18
				3.925	8	$\bar{2}$	0	4	2.232	1	2.233	13	2.237	17	0	7	16
				3.922	11	2	2	0			2.187	24B	2.196	6	0	5	18
				3.877	15	2	2	1	2.183	2			2.181	7	2	11	1
		3.84	4	3.857	20	0	1	11	2.142	3			2.143	21	0	7	17
		3.76	4	3.754	14	0	6	7			2.140	28	2.141	5	0	8	16
				3.682	5	$\bar{2}$	$\bar{2}$	5	2.126	0.5?							
3.68	9			**3.680**	**70**	0	7	5			2.098	4					
		3.66	**68B**	3.645	17	2	3	2			2.056	13	2.058	11	0	8	17
3.63	4			3.628	26	$\bar{2}$	$\bar{3}$	4					2.051	5	0	4	20
				3.569	17	0	0	$\bar{12}$	**2.049**	**6**	2.045	13	**2.047**	**66**	$\bar{4}$	0	2
				3.541	5	0	1	$\bar{12}$			2.035	22	2.036	11	0	14	1
3.54	**6**	3.54	26	3.539	11	2	1	5	2.020	2	2.015	23	2.017	12	0	14	3
				3.509	10	$\bar{2}$	$\bar{1}$	7			1.975	8	1.970	9	2	7	15
		3.47	4	3.460	15	0	8	3			1.955	8B	1.956	8	$\bar{2}$	7	17
3.45	2			3.453	6	2	4	2			1.893	25	1.895	15	2	6	17
		3.44	8B	3.439	11	$\bar{2}$	$\bar{4}$	4					1.881	13	$\bar{2}$	6	19
				3.383	7	0	8	4			1.874	12B	1.869	12	0	13	12
3.37	2	3.37	4	3.379	5	2	4	3					1.825	4	$\bar{4}$	$\bar{2}$	12
3.26	10	**3.25**	**100**	**3.272**	**48**	0	1	13					1.825	4	4	4	7
				3.243	26	0	7	8					1.824	4	$\bar{2}$	14	1
3.19	0.5	3.19	5	3.185	10	2	2	7					1.824	5	$\bar{2}$	9	17
				3.156	10	$\bar{2}$	$\bar{2}$	9			**1.819**	**46B**	1.814	6	$\bar{2}$	12	12
3.09	2	3.1	7	3.095	5	0	9	3			1.784	17	1.786	12	$\bar{4}$	$\bar{7}$	7
				3.041	7	0	1	14					1.728	10	$\bar{4}$	1	15
3.03	5	3.03	27B	3.025	17	2	5	5			1.706	28	1.710	11	0	1	25
				3.006	15	$\bar{2}$	$\bar{5}$	7			1.669	7	1.670	8	0	16	9
2.965	**6**			**2.968**	**43**	0	8	8			1.632	12B					
		2.959	27	2.958	11	2	1	9			1.382	12					
				2.932	25	2	5	6			1.342	10B					
				2.929	13	$\bar{2}$	1	11			1.238	15					

B: broad; ?: unindexed line. * Jambor (1967b). Bold-face font: main powder-diffraction lines. Values of *d* are expressed in Å.

TABLE 7. COMPARISON OF STERRYITE FROM MADOC AND Pb–Ag SULFOSALTS FROM POLLONE

		Cu	Ag	Pb	Sb	As	S	Total
				Madoc, Ontario				
Sterryite	(a) M1	tr.	<0.5	44.5	21	5.5	21.5	92.5
	(a) M2	n.d.	n.d.	47	23	6	20.5	96.5
	(b) M-35891	0.76	3.7	45.7	21.6	6.4	20.7	98.9
	(b) M-35894	0.76	3.1	46.5	22.3	5.5	20.6	98.8
	(b) NMC 61066	0.86	3.39	45.43	22.63	6.18	20.76	99.25
	(c) M-35891	0.70	3.53	45.80	22.50	6.50	20.93	99.96
	(c) M-35894	0.90	3.14	46.92	23.26	5.77	20.57	100.56
	Mean of 5 (b + c)	0.80	3.37	46.07	22.46	6.07	20.71	99.49
	σ	0.08	0.26	0.62	0.60	0.42	0.14	0.75
				Pollone, Italy				
Sb-rich sterryite		1.27	2.19	44.76	24.71	5.33	20.47	100.10*
Sb-poor sterryite		0.73	4.12	44.58	20.84	8.27	20.92	99.47
Parasterryite		0.09	4.36	47.00	19.57	7.73	20.56	99.46§
Owyheeite	(d) 1	–	5.01	46.07	26.80	1.76	19.15	98.79
	(d) 2	–	6.07	46.60	26.32	1.84	19.33	100.16

(a) Jambor (1967b), (b) Jambor *et al.* (1982), (c) Moëlo (1983), (d) Carmignani *et al.* (1976). * With minor Hg, Bi, Tl (Table 5a); § with minor Hg (Table 2a); tr.: traces, n.d.: not determined.

sulfosalts from Madoc with unknown crystal structures (madocite, launayite, playfairite, sorbyite: Jambor 1967a, 1967b), which would explain their extreme rarity in nature. Thus sterryite is a multicomponent compound belonging to the pseudosenary system PbS–Sb_2S_3–As_2S_3–Ag_2S–Cu_2S–AsS, whereas parasterryite belongs to the "simpler" pseudoquaternary system PbS–Sb_2S_3–As_2S_3–Ag_2S.

Figure 6 represents the projection of the compositions of sterryite and parasterryite (electron-microprobe data and ideal formulas), compared to various lead sulfosalts, in the pseudoternary system Pb_2S_2–$(Sb,As)_2S_3$–$(Ag,Cu)_2S$ [equivalent to the system Pb–(Sb,As)–(Ag,Cu)]. The closest minerals are Pb–Ag sulfosalts: the owyheeite solid-solution field, rathite and uchuchaccuaite. This last species is the member of the andorite series (Moëlo *et al.* 1989) poorest in Ag and Sb, but it needs some Mn together with Pb for its formation (ideal formula $AgMnPb_3Sb_5S_{12}$: Moëlo *et al.* 1984). Without Mn, the closest member of this series is fizélyite, $Ag_5Pb_{14}Sb_{21}S_{48}$.

The comparison of parasterryite with the join owyheeite–rathite is more interesting. If the unit formula of an owyheeite building block (with a periodicity of 8 Å) is subtracted from the building block of parasterryite, one gets:

$$Ag_4Pb_{20}(Sb_{14.5}As_{9.5})_{\Sigma 24}S_{58} - Ag_3Pb_{10}Sb_{11}S_{28} = AgPb_{10}(Sb_{3.5}As_{9.5})_{\Sigma 13}S_{30} \quad (1).$$

Thallium-free rathite has the ideal composition $Ag_2Pb_{12}As_{18}S_{40}$ (Berlepsch *et al.* 2002); on the basis of S = 30 atoms, it becomes $Ag_{1.5}Pb_9As_{13.5}S_{30}$, *i.e.*, a derivative of formula (1) if 1 Pb is replaced by 0.5 Ag + 0.5 As. Thus parasterryite can be considered as a rather perfect mixture of owyheeite and rathite.

In terms of Figure 6, note that 1) owyheeite has been observed in equilibrium with acicular Pb–Sb sulfosalts (boulangerite and jamesonite: Moëlo *et al.* 1984), without sterryite or parasterryite, which have an intermediate composition. This finding signifies that As is necessary for the stabilization of these two species. Moreover, parasterryite is probably an intermediate compound between owyheeite and rathite in the phase equilibrium of the pseudoquaternary system PbS–Sb_2S_3–As_2S_3–Ag_2S. 2) The ideal formula proposed for owyheeite, $Pb_{10-2x}Sb_{11+x}Ag_{3+x}S_{28}$, takes into account only the Ag-rich side of its solid-solution field (vertical bar in the ellipse of Fig. 6: Moëlo *et al.* 1984). As its Ag-poor side extends toward the compositions of sterryite and parasterryite, it is possible that this Ag-poor side corresponds to a nanoscale syntactic intergrowth of lamellae of one of these homologous derivatives in a matrix of ideal, Ag-rich owyheeite.

Conclusions

Parasterryite constitutes a complex homeotypic derivative of sterryite, with minor but significant crystal-chemical differences, among which a higher

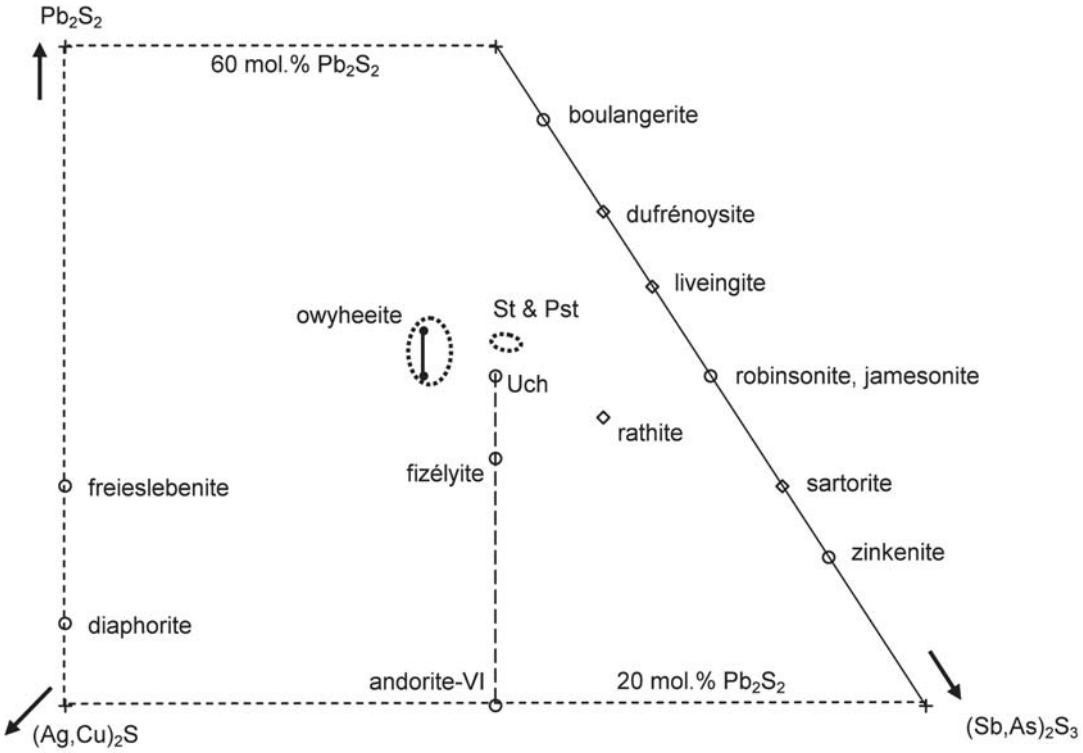

FIG. 6. Projection in the pseudoternary system Pb_2S_2–$(Ag,Cu)_2S$–$(Sb,As)_2S_3$ of the area (small ellipse) including microprobe data (from Table 7) and the ideal compositions of sterryite (St) and parasterryite (Pst). Comparison with neighboring Pb–Sb (acicular), Pb–As–(Ag) and Pb(Mn)–Ag–Sb sulfosalts. Uch.: uchucchacuaite. The larger ellipse corresponds to the solid-solution field of owyheeite, and the small vertical bar, to its ideal structural formula (Moëlo *et al*. 1984).

silver content (without Cu) and a distinct space-group in the monoclinic system. These two species are expanded homologues of owyheeite. In the Pollone mine, a more detailed sampling would be necessary to understand the paragenetic evolution, in order to define the stage(s) of formation of these two sulfosalts, and their genetic relationships with other sulfosalts, especially owyheeite, also observed in this deposit (Carmignani *et al*. 1976).

With the discovery of sterryite and the new species parasterryite at the Pollone mine, the ore deposit field of southern Apuan Alps constitutes one of the most complex districts regarding the variety of lead sulfosalts (Table 8): more than 30 species occur there, of which eight were defined in this area. Such a complexity is due principally to the association of Pb with various metals (Cu, Fe, Ag, Hg, Tl) together with Sb (major), As (frequent) or Bi (rare), and minor anions (Cl and O). From one deposit to one another, and also within a single deposit, small changes in such a complex ore composition have led to the formation of quite distinct lead sulfosalts. This gives hope of the discovery of rare or new sulfosalt species in the near future.

ACKNOWLEDGEMENTS

Electron-microprobe analyses were performed with the help of O. Rouer (CNRS engineer, Institut des Sciences de la Terre d'Orléans). We are grateful to amateur mineralogists Stefano Magnanelli and Simone Pardini, who kindly gave us the first samples of parasterryite and sterryite, respectively. We also thank Emil Makovicky and an anonymous reviewer for their constructive comments, as well as Associate Editor Allen R. Pratt. The careful editorial handling by Robert F. Martin is also greatly appreciated.

REFERENCES

BENVENUTI, M., BRIZZI, G. & DINI, A. (1993a): La miniera piombo-argentifera del Bottino (LU) (2a parte). *Riv. Mineral. Ital*. **17**, 1-22.

TABLE 8. LEAD SULFOSALTS FROM THE ORE-DEPOSIT FIELD OF SOUTH APUAN ALPS

Species	Major cations	Minor cations	Minor anions	Deposit
Aikinite	Pb – Cu – Bi			Carrara [1]
Andorite *s.l.*	Pb – Ag – Sb			Buca della Vena [2], Monte Arsiccio*[1]
Baumhauerite	Pb – As	Sb		Seravezza [1]
Boulangerite	Pb – Sb			Bottino [3], Pollone[1], Buca della Vena [2], Fornovolasco [4], Monte Arsiccio[1], Frigido [5], Carrara, Massa, Seravezza [1]
Bournonite	Pb – Sb – Cu			Bottino [3], Pollone[1], Buca della Vena [2], Fornovolasco [4]; Monte Arsiccio[1]; Carrara, Massa, Seravezza [1]
Chabournéite	Pb – Sb – Tl	As		Monte Arsiccio [6]
Cosalite	Pb – Bi			Carrara [1]
Dadsonite	Pb – Sb		Cl	Buca della Vena [7]
Diaphorite	Ag – Pb – Sb			Pollone [8]
Geocronite	Pb – Sb	As		Pollone [9]
Guettardite	Pb – Sb	As		Seravezza [1]
Izoklakeite	Pb – Bi – Sb	Ag – Cu		Seravezza [7]
Jamesonite	Pb – Sb	Fe		Fornovolasco [10], Monte Arsiccio[1]
Jaskólskiite	Pb – Sb	Cu – Bi		Fornovolasco [4]
Jordanite	Pb – As	Sb		Carrara, Seravezza [1], Pollone[1]
Marrucciite	Pb – Sb	Hg		Buca della Vena (TL) [11]
Meneghinite	Pb – Sb	Cu		Bottino (TL) [3], Fornovolasco [4], Frigido [5]
Moëloite	Pb – Sb		S excess	Seravezza (TL), Carrara, Massa [1]
Owyheeite	Pb – Sb	Ag		Pollone [12]
Parasterryite	Pb – Sb – As	Ag		Pollone (TL) [13]
Pellouxite	Pb – Sb	Ag – Cu	O – Cl	Buca della Vena (TL) [2]
Pillaite	Pb – Sb		O – Cl	Buca della Vena (TL) [2]
Robinsonite	Pb – Sb			Seravezza [1]
Rathite	Pb – As	Ag – (Sb)		Pollone[1]
Rouxelite	Pb – Sb	Cu – Hg	O	Buca della Vena (TL) [14]
Sartorite	Pb - As	Sb		Seravezza [1]
Scainiite	Pb – Sb		O	Buca della Vena (TL) [2]
Seligmannite	Pb – As – Cu			Carrara, Seravezza [1]
Semseyite	Pb – Sb			Carrara, Seravezza, Massa [1]
Sterryite	Pb – Sb	Ag – Cu – As		Pollone [13]
Zinkenite	Pb – Sb	(Cu, As)		Buca della Vena [2], Monte Arsiccio[1], Frigido [5], Seravezza, Carrara, Massa [1]

*: Andorite VI . TL: Type locality. [1]: unpublished data. References: [1] Orlandi & Criscuolo (2009), [2] Orlandi & Dini (2004), [3] Benvenuti *et al.* (1993a, 1993b), [4] Biagioni *et al*. (2008), [5] Carrozzini *et al.* (1993), [6] Bonaccorsi *et al.* (2010), [7] Orlandi *et al.* (2010), [8] Frizzo & Simone (1995), [9] D'Achiardi (1902), [10] Orlandi *et al.* (2008), [11] Orlandi *et al.* (2007), [12] Carmignani *et al.* (1976), [13] this work, [14] Orlandi *et al.* (2005).

Benvenuti, M., Brizzi, G. & Dini, A. (1993b): La miniera piombo-argentifera del Bottino (LU) (3a parte). *Riv. Mineral. Ital.* **17**, 103-119.

Benvenuti, M., Lattanzi, P., Tanelli, G. & Cortecci, C. (1986): The Ba–Fe–pyrite deposit of Buca della Vena, Apuan Alps, Italy. *Rend. Soc. Ital. Mineral. Petrol.* **41**, 347-358.

Berlepsch, P., Armbruster, T. & Topa, D. (2002): Structural and chemical variations in rathite, $Pb_8Pb_{4-x}(Tl_2As_2)_x(Ag_2As_2)As_{16}S_{40}$: modulations of a parent structure. *Z. Kristallogr.* **217**, 581-590.

Biagioni, C., Orlandi, P. & Bonini, M. (2008): Fornovolasco. Storia e miniere di ferro presso Vergemoli (Alpi Apuane). *Riv. Mineral. Ital.* **32**, 230-252.

Bonaccorsi, E., Biagioni, C., Moëlo, Y. & Orlandi, P. (2010): Chabournéite from Monte Arsiccio mine (Apuan Alps, Tuscany, Italy): occurrence and crystal structure. *Int. Mineral. Assoc., 20th Gen. Meeting* (*Budapest*), *Abstr. Ser.* **6**, 714.

Bonazzi, P., Lampronti, G.I., Bindi, L. & Zanardi, S. (2005): Wakabayashilite, $[(As,Sb)_6S_9][As_4S_5]$: crystal structure, pseudosymmetry, twinning, and revised chemical formula. *Am. Mineral.* **90**, 1108-1114.

Brizzi, G. & Olmi, F. (1989): La proustite della miniera del Pollone – Valdicastello (Lu). *Riv. Mineral. Ital.* **13**, 157-162.

Carmignani, L., Dessau, G. & Duchi, G. (1975): Una mineralizzazione sin-tettonica: il giacimento di Valdicastello (Alpi Apuane). Rapporti tra tettonica e minerogenesi in Toscana. *Boll. Soc. Geol. Ital.* **94**, 725-758.

CARMIGNANI, L., DESSAU, G. & DUCHI, G. (1976): I giacimenti a barite, pirite ed ossidi di ferro del Alpi Apuane. Studio minerogenetico e strutturale. Nuove osservazioni sui giacimienti polimetallici. *Boll. Soc. Geol. Ital.* **95**, 1009-1061.

CARMIGNANI, L. & KLIGFIELD, R. (1990): Crustal extension in the northern Apennines: the transition from compression to extension in the Alpi Apuane core complex. *Tectonics* **9**, 1275-1303.

CARROZZINI, B., GARAVELLI, C.L. & VURRO, F. (1993): Zinkenite and associated sulfides and sulfosalts from the Frigido mine (Apuane Alps). *Per. Mineral.* **62**, 13-28.

CIARAPICA, G., OLIVERO, S. & PASSERI, L. (1985): Inquadramento geologico delle principali mineralizzazioni apuane ed indizi a favore di una metallogenesi triassica. *L'Industria Mineraria* **1/1985**, 19-37.

COSTAGLIOLA, P., BENVENUTI, M., LATTANZI, P. & TANELLI, G. (1998): Metamorphogenic barite–pyrite (Pb–Zn–Ag) veins at Pollone, Apuane Alps, Tuscany: vein geometry, geothermobarometry, fluid inclusions and geochemistry. *Mineral. Petrol.* **62**, 29-60.

COSTAGLIOLA, P., BENVENUTI, M., TANELLI, G., CORTECCI, C. & LATTANZI, P. (1990): The barite–pyrite–iron oxides deposit of Monte Arsiccio (Apuane Alps). Geological setting, mineralogy, fluid inclusions, stable isotopes and genesis. *Boll. Soc. Geol. Ital.* **109**, 267-277.

D'ACHIARDI, G. (1902): Geocronite di Val di Castello presso Pietrasanta (Toscana). *Atti Soc. Tosc. Sci. Nat., Mem.* **18**, 35-48.

FRIZZO, P. & SIMONE, S. (1995): Diaphorite in the Pollone ore deposit (Apuan Alps, Tuscany, Italy). *Eur. J. Mineral.* **7**, 705-708.

JAMBOR, J.L. (1967a): New lead sulfoantimonides from Madoc, Ontario. 1. *Can. Mineral.* **9**, 7-24.

JAMBOR, J.L. (1967b): New lead sulfoantimonides from Madoc, Ontario. 2. Mineral descriptions. *Can. Mineral.* **9**, 191-213.

JAMBOR, J.L., LAFLAMME, J.H.G. & WALKER, D.A. (1982): A re-examination of the Madoc sulfosalts. *Mineral. Rec.* **13**, 93-100.

KERNDT, T. (1845): Über die Krystallform und die chemische Zusammensetzung des Geokronits von Val di Castello. *Ann. Phys.* **141**, 302-307.

KLIGFIELD, R., HUNZIKER, J., DALLMEYER, R.D. & SCHAMEL, S. (1986): Dating of deformation phases using K–Ar and $^{40}Ar/^{39}Ar$ techniques: results from the northern Apennines. *J. Struct. Geol.* **8**, 781-798.

LATTANZI, P., BENVENUTI, M., COSTAGLIOLA, P. & TANELLI, G. (1994): An overview on recent research on the metallogeny of Tuscany with special reference to the Apuane Alps. *Mem. Soc. Geol. Ital.* **48**, 613-625.

LAUFEK, F., PAŽOUT, R. & MAKOVICKY, E. (2007): Crystal structure of owyheeite, $Ag_{1.5}Pb_{4.43}Sb_{6.07}S_{14}$: refinement from powder synchrotron X-ray diffraction. *Eur. J. Mineral.* **19**, 557-566.

MAKOVICKY, E. (1985): Cyclically twinned sulphosalt structures and their approximate analogues. *Z. Kristallogr.* **173**, 1-23.

MOËLO, Y. (1983): Contribution à l'étude des conditions naturelles de formation des sulfures complexes d'antimoine et plomb. *Doc. BRGM* **57**, Orléans, France.

MOËLO, Y., MAKOVICKY, E. & KARUP-MØLLER, S. (1989): Sulfures complexes plombo-argentifères: minéralogie et cristallochimie de la série andorite–fizélyite. *Doc. BRGM* **167**, Orléans, France.

MOËLO, Y., MAKOVICKY, E., MOZGOVA, N.N., JAMBOR, J.L., COOK, N., PRING., A., PAAR, W.H., NICKEL, E.H., GRAESER, S., KARUP-MØLLER, S., BALIĆ-ŽUNIĆ, T., MUMME, W.G., VURRO, F., TOPA, D., BINDI, L., BENTE, K. & SHIMIZU, M. (2008): Sulfosalt systematics: a review. Report of the sulfosalt sub-committee of the IMA Commission on Ore Mineralogy. *Eur. J. Mineral.* **20**, 7-46.

MOËLO, Y., MOZGOVA, N., PICOT, P., BORTNIKOV, N. & VRUBLEVSKAYA, Z. (1984): Cristallochimie de l'owyheeite: nouvelles données. *Tschermaks Mineral. Petrogr. Mitt.* **32**, 271-284.

MOËLO, Y., OUDIN, E., PICOT, P. & CAYE, R. (1984): L'uchucchacuaïte, $AgMnPb_3Sb_5S_{12}$, une nouvelle espèce minérale de la série de l'andorite. *Bull. Minéral.* **107**, 597-604.

MULLEN, D.J.E. & NOWACKI, W. (1972): Refinement of the crystal structure of realgar AsS and orpiment, As_2S_3. *Z. Kristallogr.* **136**, 48-65.

ORLANDI, P. & CRISCUOLO, A. (2009): *Minerali del marmo delle Alpi Apuane. Parco delle Alpi Appuane*. Pacini, Ospedaletto, Pisa, Italy.

ORLANDI, P. & DINI, A. (2004): Die Mineralien der Buca della Vena-mine, Apuaner Berge, Toskana (Italien). *Lapis* **29**, 11-24.

ORLANDI, P., MEERSCHAUT, A., MOËLO, Y., PALVADEAU, P. & LÉONE, P. (2005): Lead–antimony sulfosalts from Tuscany (Italy). VIII. Rouxelite, $Cu_2HgPb_{22}Sb_{28}S_{64}(O,S)_2$, a new sulfosalt from Buca della Vena mine, Apuan Alps: definition and crystal structure. *Can. Mineral.* **43**, 919-933.

ORLANDI, P., MOËLO, Y. & BIAGIONI, C. (2008): Jamesonite delle miniere di Fornovolasco (Vergemoli, Lucca): primo ritrovamento sulle Alpi Apuane. *Atti Soc. Tosc. Sci. Nat., Mem., Ser. A* **113**, 89-95.

ORLANDI, P., MOËLO, Y. & BIAGIONI, C. (2010): Lead–antimony sulfosalts from Tuscany (Italy). X. Dadsonite from the Buca della Vena mine and Bi-rich izoklakeite from the Seravezza marble quarries. *Per. Mineral.* **79**, 113-121.

ORLANDI, P., MOËLO, Y., CAMPOSTRINI, I. & MEERSCHAUT, A. (2007): Lead–antimony sulfosalts from Tuscany (Italy). IX. Marrucciite, $Hg_3Pb_{16}Sb_{18}S_{46}$, a new sulfosalt from Buca della Vena mine, Apuan Alps: definition and crystal structure. *Eur. J. Mineral.* **19**, 267-279.

ORLANDI, P., MOËLO, Y., MEERSCHAUT, A. & PALVADEAU, P. (1999): Lead–antimony sulfosalts from Tuscany (Italy). I. Scainiite, $Pb_{14}Sb_{30}S_{54}O_5$, the first Pb–Sb oxy-sulfosalt, from Buca della Vena mine. *Eur. J. Mineral.* **11**, 949-954.

ORLANDI, P., MOËLO, Y., MEERSCHAUT, A. & PALVADEAU, P. (2001): Lead–antimony sulfosalts from Tuscany (Italy). III. Pillaite, $Pb_9Sb_{10}S_{23}ClO_{0.5}$, a new Pb–Sb chloro-sulfosalt, from Buca della Vena mine. *Eur. J. Mineral.* **13**, 605-610.

ORLANDI, P., MOËLO, Y., MEERSCHAUT, A., PALVADEAU, P. & LÉONE, P. (2004): Lead–antimony sulfosalts from Tuscany (Italy). VI. Pellouxite, $\sim(Cu,Ag)_2Pb_{21}Sb_{23}S_{55}ClO$, a new oxy-chloro-sulfosalt from Buca della Vena mine, Apuan Alps. *Eur. J. Mineral.* **16**, 839-844.

PANDELI, E., BAGNOLI, P. & NEGRI, M. (2004): The Fornovolasco schists of the Apuan Alps (northern Tuscany, Italy): a new hypothesis for their stratigraphic setting. *Boll. Soc. Geol. Ital.* **123**, 53-66.

Received September 22, 2010, revised manuscript March 5, 2011.